Journal of Zhejiang University-SCIENCE A (Applied Physics & Engineering)
ISSN 1673-565X (Print); ISSN 1862-1775 (Online)
www.jzus.zju.edu.cn; www.springerlink.com
E-mail: jzus@zju.edu.cn

Bayesian operational modal analysis of a long-span cable-stayed sea-crossing bridge*

Yan-long XIE[1,2], Binbin LI[1,2], Jian GUO[†‡3]

[1]*ZJU-UIUC Institute, Zhejiang University, Haining 314400, China*

[2]*College of Civil Engineering and Architecture, Zhejiang University, Hangzhou 310058, China*

[3]*College of Civil Engineering and Architecture, Zhejiang University of Technology, Hangzhou 310023, China*

[†]E-mail: guoj@zjut.edu.cn

Received Oct. 10, 2019; Revision accepted Feb. 11, 2020; Crosschecked June 15, 2020

Abstract: Sea-crossing bridges have attracted considerable attention in recent years as an increasing number of projects have been constructed worldwide. Situated in the coastal area, sea-crossing bridges are subjected to a harsh environment (e.g. strong winds, possible ship collisions, and tidal waves) and their performance can deteriorate quickly and severely. To enhance safety and serviceability, it is a routine process to conduct vibration tests to identify modal properties (e.g. natural frequencies, damping ratios, and mode shapes) and to monitor their long-term variation for the purpose of early-damage alert. Operational modal analysis (OMA) provides a feasible way to investigate the modal properties even when the cross-sea bridges are in their operation condition. In this study, we focus on the OMA of cable-stayed bridges, because they are usually long-span and flexible to have extremely low natural frequencies. It challenges experimental capability (e.g. instrumentation and budgeting) and modal identification techniques (e.g. low frequency and closely spaced modes). This paper presents a modal survey of a cable-stayed sea-crossing bridge spanning 218 m+620 m+218 m. The bridge is located in the typhoon-prone area of the northwestern Pacific Ocean. Ambient vibration data was collected for 24 h. A Bayesian fast Fourier transform modal identification method incorporating an expectation-maximization algorithm is applied for modal analysis, in which the modal parameters and associated identification uncertainties are both addressed. Nineteen modes, including 15 translational modes and four torsional modes, are identified within the frequency range of [0, 2.5 Hz].

Key words: Cable-stayed sea-crossing bridge; Operational modal analysis (OMA); Bayesian modal identification; Expectation-maximization (EM) algorithm

https://doi.org/10.1631/jzus.A1900511 **CLC number:** U441.3

1 Introduction

In recent years, an increasing number of sea-crossing bridges have been built worldwide. They are constructed for the purpose of promoting the transportation network and economic development of coastal areas. Compared to cross-river bridges, sea-crossing bridges are often subjected to harsher environmental conditions (Guo, 2010). Wind is one of the dominant loadings that causes vibrations (e.g. flutter and vortex), especially for those typhoon-prone areas (Zhou and Sun, 2018; Xu et al., 2019). Seismic risk is another issue occurring more often because of the movements and collisions between the continental and oceanic plate margins (Li et al., 2018). Wave and wave current induce hydrodynamic problems further affecting structural bearing capacity (Liu, 2006).

To ensure the safety and serviceability of sea-crossing bridges, structural health monitoring (SHM)

‡ Corresponding author

* Project supported by the Start-up Fund from Zhejiang University (No. 130000-171207704/018) and the National Natural Science Foundation of China (Nos. U1709207, 51578506, and 51908494)

ORCID: Jian GUO, https://orcid.org/0000-0003-3605-2999

systems are employed to monitor the structural response and provide information on the health states (e.g. level of damage) of bridges. Vibration-based techniques have been widely applied to identify structural damage. Here the data is generally processed through Fourier transform or wavelet transform (Doebling et al., 1998; Ren and de Roeck, 2002; Kim and Melhem, 2004; Guo et al., 2005; Taha et al., 2006). The structural modal parameters (e.g. modal frequencies, damping ratios, and mode shapes) are often used as the indicators of health state. Challenges exist since the modal information is not sensitive enough to the structural damage, and the variation of the parameters can be due to environmental and operational changes rather than the damage (Zhou and Sun, 2019). From the authors' experience/view, several things need to be clarified in the SHM community. Firstly, more attention should be paid to the overall structural health state, which can be quantified by the failure probability with formulating appropriate limit state functions, instead of examination of any superficial damage. The damage that cannot be detected by the change of modal parameters may have negligible effect on the failure probability. Secondly, although the modal parameters are important factors to consider in the SHM, we should not be overoptimistic of its role. For instance, it is unrealistic to locate the damage of a kilometer-long bridge by deploying only several accelerometers. As for the variability of modal parameters, a large data set as the reference state is necessary and the data should be analyzed in a probabilistic manner. Besides the demands for the SHM, it is of great interest to investigate the structural modal properties of sea-crossing bridges for the purpose of validating and updating their numerical models in the design stage as well as understanding their dynamic behavior.

Operational modal analysis (OMA), also known as ambient modal identification, aims at identifying structural modal properties using output-only data (Brincker and Ventura, 2015). The excitation in OMA is commonly unmeasured but assumed to be 'broadband random'. Since it does not require specific knowledge of input and thus is economic in implementation, OMA has attracted considerable attention in the vibration testing of civil engineering structures. Identification techniques can be generally distinguished by the format of data either in the time domain or in the frequency domain. Though there are time-frequency domain methods, their applications are rare and thus not introduced here. In the time domain, representative methods include Ibrahim time domain method (Ibrahim, 1977) and stochastic subspace identification (SSI) with its variants (Peeters and de Roeck, 2001). The SSI methods have been widely used in OMA applications as they are robust and efficient (Mevel et al., 2003; Brownjohn et al., 2010; Liu et al., 2013). In addition, automated OMA techniques using a multi-stage clustering approach allow the modal identification to be performed without user interactions, and this greatly facilitates data analysis (Reynders et al., 2012; Sun et al., 2017). As for frequency domain methods, peak-picking (Felber, 1993) and frequency domain decomposition (FDD) (Brincker et al., 2000) are popular. Because of the frequency nature of modal parameters and the existence of the fast Fourier transform (FFT), frequency domain methods exhibit great efficiency in processing long-time stationary data, while the time domain methods have the advantage of dealing with nonstationary and transient data.

Although the identification of natural frequency and mode shape usually has adequate accuracy, the precision of estimating damping is still insufficient (Zhang et al., 2005). In order to quantify the identification uncertainties, statistics-based OMA methods have been developed. Working with classical statistics (or the frequentist approach), various estimators (Brincker and Ventura, 2015) have been proposed to infer modal parameters, whose uncertainty arises from the uncertain data. Different from the 'frequentist' point of view, the Bayesian method represents another school of thought. It views the problem as a posterior inference, and all the knowledge of modal parameters is encapsulated in their joint posterior distribution (Au et al., 2013). The Bayesian method identifies the structural modal properties as the most probable values (MPVs) and provides identification uncertainties by the posterior covariance matrix. The Bayesian FFT method is a typical approach formulated in the frequency domain. Fast algorithms for the calculation of MPV have been developed for well-separated modes (Au, 2011) and closely spaced modes (Au, 2012). An expectation-maximization

(EM) algorithm and its variants have been proposed recently, which have improved the computational efficiency and convergence (Li and Au, 2019).

In this study, a modal survey of a cable-stayed sea-crossing bridge has been conducted, where structural modal properties have been identified using the Bayesian FFT method. In this paper, a brief review of the Bayesian FFT method incorporating the EM algorithm is given first. Then, a detailed description of the bridge is provided. At last, the investigation with field data is presented.

2 Bayesian FFT with EM algorithm

Let the measured acceleration time history of n degrees of freedom (DOFs) be $\{\boldsymbol{y}_j \in \mathbb{R}^n\}_{j=0}^{N-1}$, where N is the number of samples per data channel. The (scaled) FFT of data is given by

$$\boldsymbol{F}_k = \sqrt{\Delta t/N}\sum_{j=0}^{N-1}\boldsymbol{y}_j \exp(-2\pi \mathrm{i} jk/N), \tag{1}$$

where $\mathrm{i}^2=-1$; Δt is the sampling interval; $\boldsymbol{F}_k$ corresponds to the frequency $f_k=k\Delta t/N$ up to the Nyquist frequency $N_\mathrm{q}=\mathrm{int}[N/2]$, where int[.] denotes the integer part and $k=1, 2, \ldots, N_\mathrm{q}$.

Applying the Bayes' theorem and assuming a uniform prior probability density function (PDF), the posterior PDF of modal parameters, denoted by $\boldsymbol{\theta}$, for the given FFT data $\{\boldsymbol{F}_k\}$ is proportional to the likelihood function, i.e.

$$p(\boldsymbol{\theta}\,|\,\{\boldsymbol{F}_k\}) \propto p(\{\boldsymbol{F}_k\}\,|\,\boldsymbol{\theta}), \tag{2}$$

where $p(\{\boldsymbol{F}_k\}\,|\,\boldsymbol{\theta})$ is also known as the joint PDF of $\{\boldsymbol{F}_k\}$ condition on $\boldsymbol{\theta}$. For small Δt and large N, the FFT data $\{\boldsymbol{F}_k\}$ is asymptotically independent and jointly 'circularly complex Gaussian' distributed. The likelihood function is then given by

$$p(\{\boldsymbol{F}_k\}\,|\,\boldsymbol{\theta}) = \pi^{-nN_\mathrm{f}}\prod_k |\boldsymbol{E}_k|^{-1}\exp\left[-\sum_k \boldsymbol{F}_k^* \boldsymbol{E}_k^{-1}\boldsymbol{F}_k\right], \tag{3}$$

where N_f is the number of FFT data within the selected frequency band; '*' represents the conjugate transpose; '| |' denotes the matrix determinant; $\boldsymbol{E}_k$ is the theoretical covariance matrix of $\{\boldsymbol{F}_k\}$, i.e. the expectation of $\boldsymbol{F}_k\boldsymbol{F}_k^*$.

For a classically damped system, if there are m modes dominating the selected frequency band, the FFT data can be modeled as

$$\boldsymbol{F}_k = \boldsymbol{\Phi}\boldsymbol{h}_k\boldsymbol{p}_k + \boldsymbol{\varepsilon}_k, \tag{4}$$

where $\boldsymbol{h}_k=\mathrm{diag}(h_{1k}, h_{2k}, \ldots, h_{mk})$ is a diagonal matrix with the frequency response function (FRF) being the diagonal entry; $\boldsymbol{p}_k$ is the FFT of the modal excitation; $\boldsymbol{\Phi}=[\boldsymbol{\varphi}_1, \boldsymbol{\varphi}_2, \ldots, \boldsymbol{\varphi}_m]$ is the mode shape matrix corresponding to the measured DOFs; $\boldsymbol{\varepsilon}_k$ is the prediction error consisting of channel noise and modeling error.

The FRF contains the natural frequency f and damping ratio $\boldsymbol{\zeta}$. The modal excitation $\boldsymbol{p}_k$ and prediction error $\boldsymbol{\varepsilon}_k$ are modelled as independent circularly complex Gaussian distributions with a constant power spectral density (PSD) matrix of $\boldsymbol{S}$ and a constant PSD of S_e, respectively. The theoretical covariance matrix $\boldsymbol{E}_k$ is then given by

$$\boldsymbol{E}_k = \boldsymbol{\Phi}\boldsymbol{H}_k\boldsymbol{\Phi}^\mathrm{T} + S_\mathrm{e}\boldsymbol{I}_n, \tag{5}$$

where $\boldsymbol{H}_k=\boldsymbol{h}_k\boldsymbol{S}\boldsymbol{h}_k^*$, and $\boldsymbol{I}_n$ is the $n\times n$ identity matrix.

In the above probabilistic model, the modal excitation is assumed to be broadband random, and have a constant PSD within the selected frequency band. Since this band is usually narrow, it is much more robust than the conventional 'white noise' assumption (i.e. constant PSD for all frequencies) in most OMA methods. On the other hand, the possible input loads, e.g. wind, sea-wave, and traffic load, have generally a slow-varying spectrum, so that the assumption of constant PSD within the narrow band should not induce a large modeling error. The same reasoning holds for the measurement error, because most accelerometers have a slow-varying 'pink' spectrum.

With sufficient data, the posterior distribution of modal parameters can be well approximated by a Gaussian distribution centered around the MPVs, and the covariance matrix is given by the inverse of the Hessian of the negative log-likelihood function. Computation of the MPVs and the covariance matrix is non-trivial, primarily because the number of modal

parameters can be large and the matrix $\boldsymbol{E}_k$ is almost rank-deficient when the signal-to-noise ratio is high (i.e. small S_e) and the number of modes m is fewer than that of the measured DOFs n. For the calculation of MPVs, a recently developed EM algorithm (Li and Au, 2019) has been applied in this study, and it is briefly reviewed below.

The EM algorithm takes advantage of the model structure to decouple the optimization problem into more manageable pieces. This divide-and-conquer strategy gives a conceptual clarity and simplicity of the algorithm. Instead of directly maximizing the log-likelihood function, the EM algorithm maximizes the expectation of the complete-data log-likelihood function, which is in fact a lower bound of the log-likelihood function. More specifically, consider the FFT $\boldsymbol{F}_k$ as the observed variable and the modal response $\boldsymbol{\eta}_k=\boldsymbol{h}_k\boldsymbol{p}_k$ as the latent variable. The conditional joint distribution $p(\{\boldsymbol{F}_k, \boldsymbol{\eta}_k\}|\boldsymbol{\theta})$ then gives the so-called complete-data likelihood function. In the implementation of the EM algorithm, for a given starting value $\boldsymbol{\theta}^{(0)}$, the expectation step computes the expected complete-data log-likelihood function (Q function) and the maximization step obtains the MPV of $\boldsymbol{\theta}$ by maximizing the Q function.

For the expectation step,

$$Q(\boldsymbol{\theta}|\boldsymbol{\theta}^{(t)}) = E_{\{\boldsymbol{\eta}_k\}|\{\boldsymbol{F}_k\},\boldsymbol{\theta}^{(t)}}[\log p(\{\boldsymbol{F}_k, \boldsymbol{\eta}_k\}|\boldsymbol{\theta})], \quad (6)$$

where $E[.]$ denotes the expectation operator.

For the maximization step,

$$\{\boldsymbol{\theta}^{(t+1)}\} = \arg_{\boldsymbol{\theta}} \max[Q(\boldsymbol{\theta}|\boldsymbol{\theta}^{(t)})]. \quad (7)$$

The two steps are iterated until convergence. In the developed EM algorithm, the updates of $\boldsymbol{\Phi}$, $\boldsymbol{S}$, and S_e have been derived analytically, allowing a fast calculation of MPVs. Variants of the above ordinary EM were also proposed by Li and Au (2019) to accelerate its convergence, but they will not be introduced here because of space limitations.

3 Bridge information

The investigated sea-crossing bridge is called 'Jintang Bridge', a three-span cable-stayed bridge, shown in Fig. 1. It is a part of Ningbo-Zhoushan expressway that connects Jintang Island and Ningbo City. An elevation view of the bridge is shown in Fig. 2. The main span is 620 m and there are two side spans of 218 m. The steel-box girder is 30.1 m in width with uniform cross section. In addition, the pylons were made of reinforced concrete with a height of 204 m, and the height over the deck is 155 m.

Fig. 1 Overview of the investigated cable-stayed sea-crossing bridge (Jintang Bridge)

During its operation, large amounts of data have been acquired by an SHM system installed to facilitate operation management and early alert of possible damage. Fifteen uniaxial piezoelectric accelerometers (ASP series, manufactured by KYOWA, Japan, with a sensitivity of 100 mV/g (±10%)) were permanently installed on the bridge to measure the vibration responses of the girder. Two data acquisition systems (UCAM series, KYOWA) with data recording hardware (2 GB built-in memory) were equipped at both sides of the bridge. They connected the nearby sensors and were synchronized via an internal clock. The sensor locations are graphically shown in Fig. 2 and a detailed description is provided in Table 1.

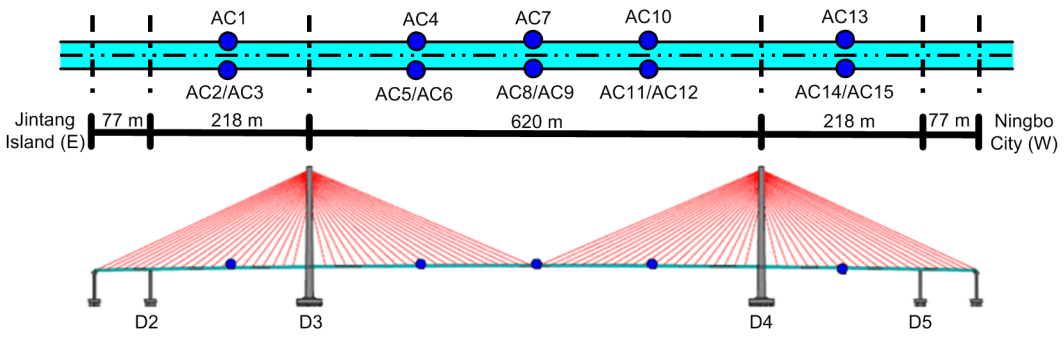

Fig. 2 Elevation view of the bridge and sensor locations

Table 1 Sensor location detail

Sensor	Direction	Location
AC1/AC3	Vertical	1/2 of (left) side-span (D2–D3)
AC2	Longitudinal	
AC4/AC6	Vertical	1/4 of the main-span (D3–D4)
AC5	Longitudinal	
AC7/AC9	Vertical	1/2 of the main-span (D3–D4)
AC8	Longitudinal	
AC10/AC12	Vertical	3/4 of the main-span (D3–D4)
AC11	Longitudinal	
AC13/AC15	Vertical	1/2 of (right) side-span (D4–D5)
AC14	Longitudinal	

4 Investigation with field data

In this study, we investigate the modal parameters of Jintang Bridge based on the data recorded at a sampling rate of 50 Hz for 24 h on July 13, 2013. A typical data set of 3600 s is shown in Fig. 3, where we can find large amplitudes of vibration for several short periods, but low vibration levels in most of the time. The data is split into 15-min segments for modal analysis. Each segment contains about 200 cycles of the fundamental mode, calculated as (measurement duration)/(fundamental period)=200, which is considered to be sufficient for modal identification with an acceptable precision (Au, 2014). The choice of the aforementioned time window also takes into account that the variation of the operation condition, e.g. temperature, can be neglected over such a short period.

In order to indicate the modes of interest and select frequency bands for modal identification, a singular value (SV) spectrum of the measured data is first viewed in Fig. 4. It is the plot of the eigenvalues of the sample PSD matrix against frequency. The bold line in the figure shows the largest eigenvalues, and the peaks indicate potential modes that display dynamic amplification. The significance of peaks over remaining lines indicates the level of signal-to-noise effect. The more significant the peaks, the higher the signal-to-noise ratio. The horizontal bars '[-]' and the circles 'o' in the figure represent the selected frequency bands and initial guesses of the natural frequency. The selection of the frequency band is a trade-off between the amount of information used in making an inference of the modal parameters and the modelling error risk. From the plot, a number of modes can be observed: the first mode is as low as 0.2 Hz and the modes are dense in the range of [0, 2.5 Hz], including several groups of closely spaced modes, which dramatically increase the difficulty for an efficient and reliable modal identification. In this study, 19 bands within 2.5 Hz are selected for modal identification. It should be mentioned that the peaks

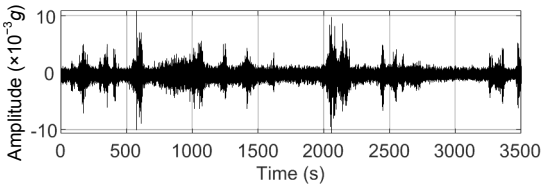

Fig. 3 Time history of a typical data set (*g* indicates the acceleration of gravity)

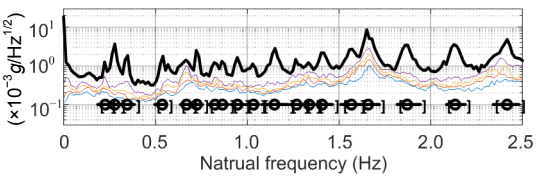

Fig. 4 SV spectrum of the measured data

of some modes are not always as obvious as shown in Fig. 4 for different data sets. This is common in practice since not all modes are well-excited consistently because of the randomness of excitation.

The modal parameters are identified using the Bayesian FFT method reviewed in Section 2, where the MPVs of the modal parameters as well as their identification uncertainties are computed for the time segment from 1:00 am to 1:15 am. In order to compare identification results, the data is also analyzed using the FDD technique. As shown in Table 2, the natural frequencies identified by FDD match well with the Bayesian FFT results. For the damping ratio estimation, discrepancies are apparent between these two methods. This is due to the fact that the identification uncertainty of the damping ratios is significantly higher than that of the natural frequencies. It should be noted that both methods operate in the frequency domain, but they have fundamental differences. The FDD only uses the information of the PSD at the modal frequencies, while the Bayesian FFT method takes advantage of the information in a frequency band containing modal frequencies. It directly models the FFT data (not the PSD) parameterized by the modal frequencies, damping ratios, and mode shapes. The constructed probabilistic model is then inferred following the Bayesian principle in an iterative way, in which the eigenvalue decomposition is not needed.

The identified MPVs and the coefficients of variation (COVs) (COV=posterior standard deviation/MPV) of modal parameters are also provided in Table 2. It is seen from the table that the posterior COVs of the natural frequency and damping ratio generally decrease with the modal frequencies. This is mainly due to the increase of the effective data length, which is defined as the data duration over the natural period. That is, more cycles of waves are used in identification as the modal frequencies increase (Au, 2014).

The frequencies are densely distributed within the low frequency band ranging from 0 to 2.5 Hz, mainly because of the long span, and thus small stiffness, of the girder. These frequencies are associated with small posterior uncertainties, indicating a reliable estimation. Except for the 8th mode, the damping ratios of the remaining modes are less than 3%, which generally follows our engineering experience, because the bridge only exhibits a small vibration amplitude in the normal operational condition. The posterior COV of the damping ratio can be as large as 28%, showing a great variability so that the identified MPVs should be used with caution. We can observe that posterior COVs of frequencies and damping ratios tend to decrease with the mode number. This is partly because the effective data length (data duration/natural period) is longer for higher modes with higher frequencies.

Table 2 Identified modal parameters

Mode	Natural frequency			Damping ratio			Mode shape	
	MPV (Hz)	COV (%)	FDD (Hz)	MPV (%)	COV (%)	FDD (%)	Pattern	COV (%)
1	0.224	0.21	0.226	0.80	28	1.92	T	8.8
2	0.274	0.19	0.275	1.00	21	1.95	V	2.7
3	0.341	0.13	0.342	0.55	26	1.26	V	4.9
4	0.539	0.14	0.543	0.82	20	1.44	V	4.7
5	0.672	0.35	0.674	2.48	20	0.42	T	9.7
6	0.727	0.07	0.726	0.27	26	0.38	V	7.1
7	0.817	0.15	0.818	0.95	15	1.63	V	8.9
8	0.850	0.29	0.867	3.03	16	1.80	T+R	5.5
9	0.944	0.11	0.958	0.84	16	1.17	V	4.8
10	1.025	0.16	1.037	1.24	17	1.09	V	7.8
11	1.151	0.10	1.153	0.90	14	0.47	V	3.2
12	1.277	0.19	1.269	1.59	19	0.35	T+R	8.3
13	1.338	0.17	1.343	1.29	20	1.50	V+R	9.5
14	1.409	0.11	1.409	0.90	16	1.02	V	5.8
15	1.567	0.10	1.587	0.93	14	0.57	V	4.4
16	1.653	0.04	1.654	0.22	19	0.50	T+V	7.8
17	1.868	0.06	1.874	0.59	13	0.91	V	3.0
18	2.130	0.07	2.154	0.68	12	0.96	V	2.2
19	2.414	0.06	2.423	0.61	12	0.95	V+R	4.6

T represents the translational mode in transverse; V represents the vertical directions; R represents the torsional mode

The mode shape COV is calculated as the trace of the posterior mode shape covariance matrix. The corresponding mode shapes are plotted in Fig. 5. It is found that the fundamental mode has a frequency of 0.224 Hz or a natural period of 4.5 s with an anti-symmetric shape in the transverse direction. Since the transverse direction of the girder is less constrained by the cables, its bending stiffness in the transverse direction is less than that in the vertical direction, which explains why the transverse mode appears first. The first vertical mode occurs at 0.274 Hz with a symmetric shape, while the anti-symmetric vertical mode appears until 0.672 Hz. Because of the effect

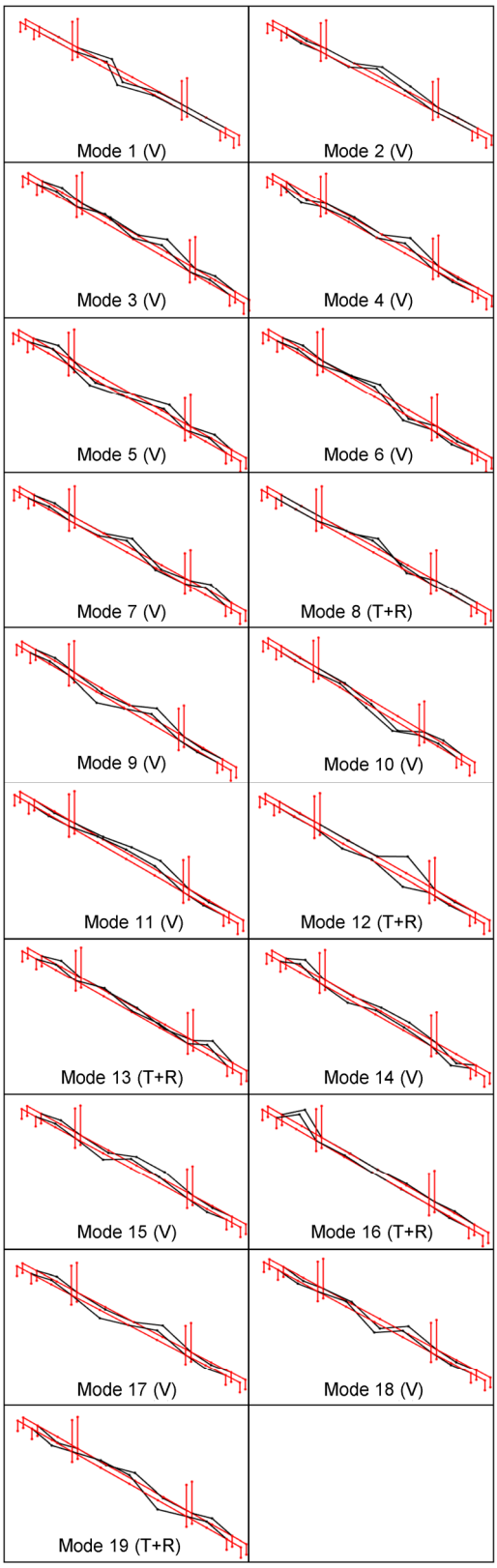

Fig. 5 Identified mode shapes. References to color refer to the online version of this figure

of cables, the mode coupling behavior occurs often, especially for those torsional modes, e.g. Modes 8, 12, 13, and 19. It should be noted that this work uses 15 accelerometers to identify 19 modes, and hence several mode shapes cannot be directly distinguished, e.g. Modes 9 and 17. This is due to the lack of adequate instruments. However, it is still possible to separate them by checking their natural frequencies and damping ratios.

The same procedures are applied to identify modal parameters for the remaining data, and the results of the natural frequency and damping ratio in 24 h are shown in Fig. 6. Black thick lines indicate the MPVs of parameters and grey areas cover ±2 posterior standard deviations. The frequencies change slightly with time, while the damping ratios have a larger variation but still are in the same order of magnitude. The time variation of modal parameters is mainly due to the randomness of the ambient excitation.

Finally, we would like to mention the efficiency of the Bayesian FFT method using the EM algorithm, because it is directly relevant to its practical applicability. For the considered example, modal parameters and their associated uncertainties are computed using a Matlab programming of the EM algorithm and run on a laptop of ThinkPad T480s (Intel Core i7, 8 GB of RAM and 512 GB of SSD). The computational time for identifying each mode is in the order of several seconds and it takes around 20 min to process the 24-h data. Since the identification is conducted in a band-wise manner, it can be easily accelerated taking advantage of the parallel computation. Owing to its efficiency and accuracy, it is ready for practical application, even in the scenario of real-time identification of structural modes.

5 Conclusions

In this study, a modal survey has been conducted on a sea-crossing cable-stayed bridge using the up-to-date Bayesian FFT method. The applied algorithm successfully identified 19 modes within [0, 2.5 Hz], including 15 translational modes and four torsional modes. The identified modes contain low frequencies, closely spaced modes, and coupled mode shapes of cable-stayed bridges, which challenge the modal

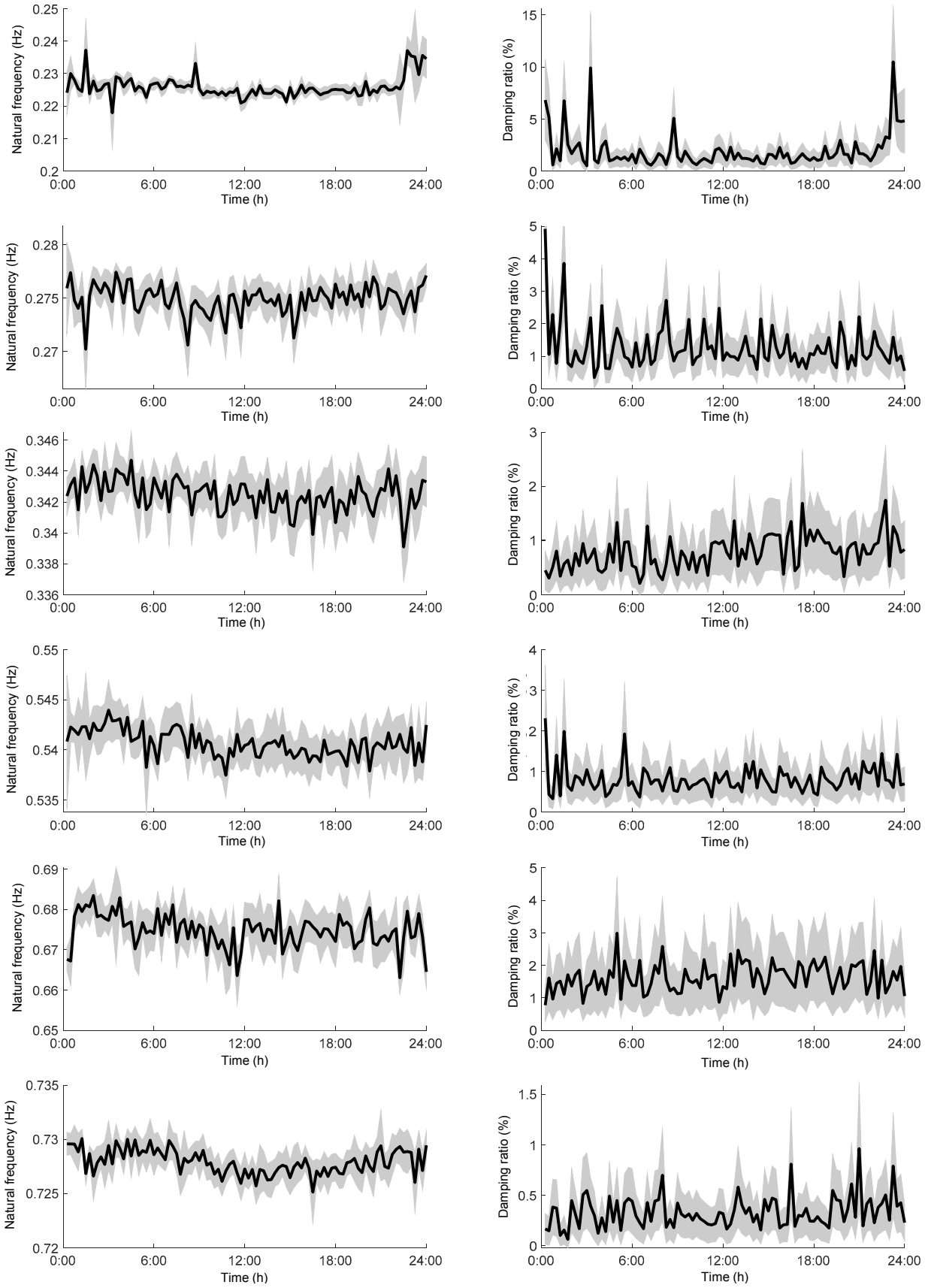
Natural frequency (Hz)
Damping ratio (%)
Time (h)
0:00
6:00
12:00
18:00
24:00

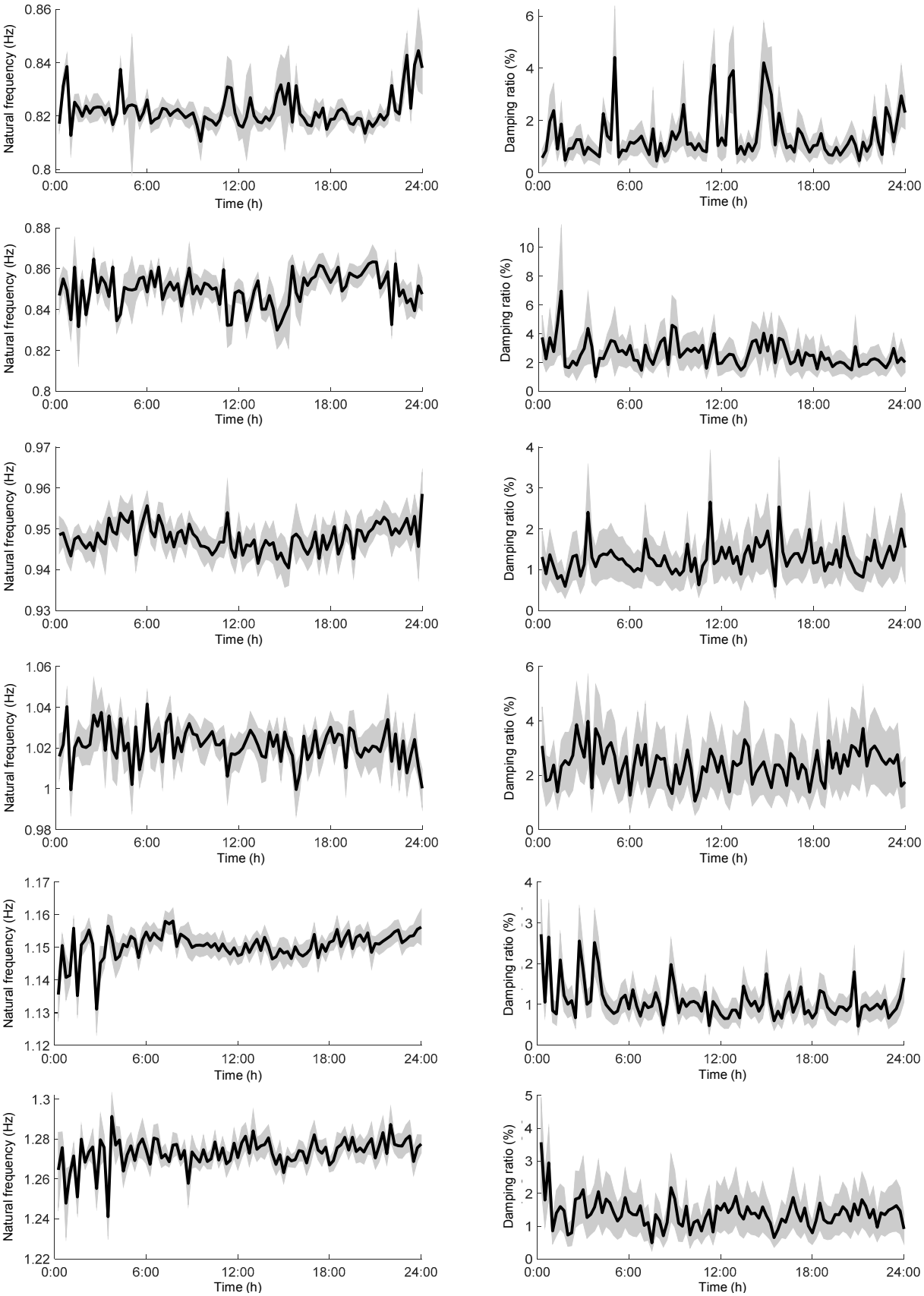
Natural frequency (Hz)
Damping ratio (%)
Time (h)
0:00
6:00
12:00
18:00
24:00

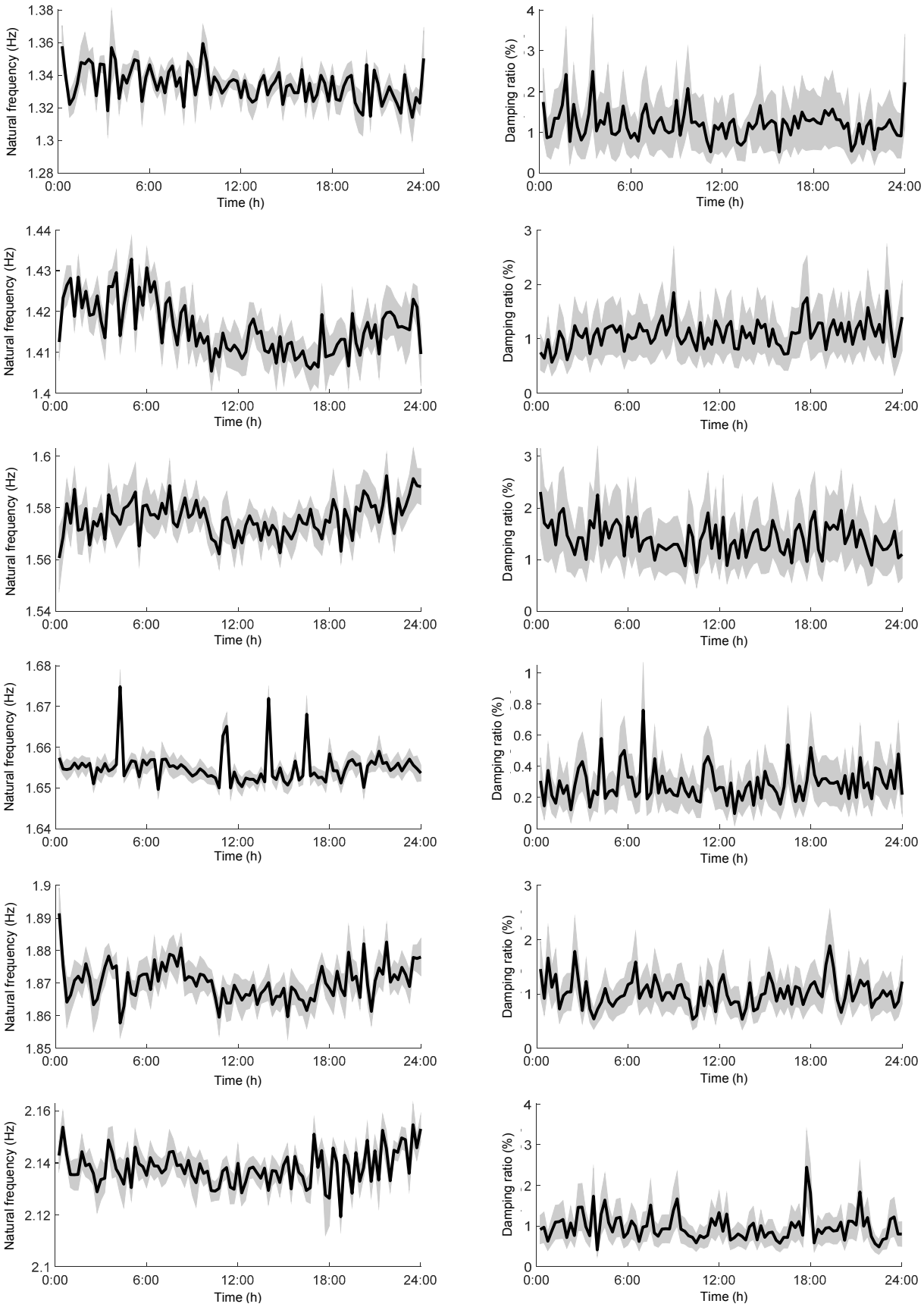
Natural frequency (Hz)
Damping ratio (%)
Time (h)
0:00
6:00
12:00
18:00
24:00

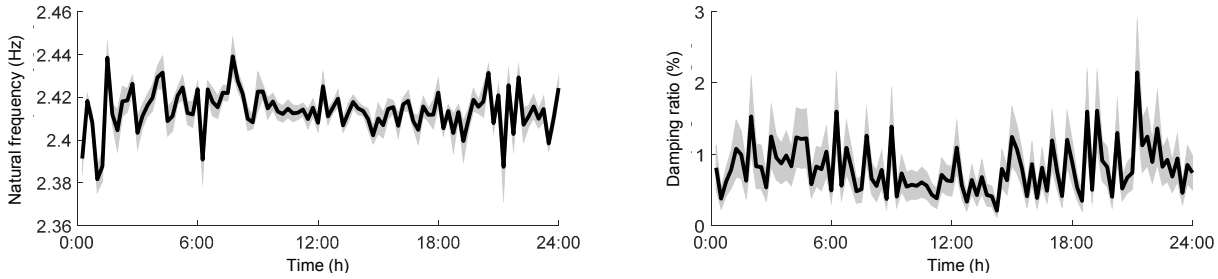

Fig. 6 Identified natural frequencies and damping ratios of Modes 1–19 with 24-h data (black thick lines indicate the MPVs and grey areas cover ±2 posterior standard derivations)

identification techniques. This study demonstrates that the Bayesian FFT method is applicable for identifying modal parameters of long-span sea-crossing bridges with adequate accuracy and efficiency. The identification results show that, due to the constraints of cables, the mode shapes of cable-stayed bridges are significantly different from those of beam bridges, and it is important to monitor the vibration of the girder. The identified modal parameters serve as a baseline value for the monitoring of Jintang Bridge.

The significance of this study lies in providing a feasible way of investigating the dynamic behavior of cable-stayed sea-crossing bridges. The result could potentially be used to update the numerical model and to detect structural damage. Although the Bayesian FFT method provides an efficient and reliable way to identify modal parameters as well as the associated identification uncertainties, analyzing the data still requires hand-picking of the frequency bands and the initial guesses of the natural frequencies. In this sense, developing an automated Bayesian FFT technique will greatly facilitate its use in the SHM field.

Contributors

Jian GUO designed the research and collected the data. Yan-long XIE processed the data and wrote the first draft of the manuscript. Binbin LI helped to organize the manuscript and revised the final version.

Conflict of interest

Yan-long XIE, Binbin LI, and Jian GUO declare that they have no conflict of interest.

References

Au SK, 2011. Fast Bayesian FFT method for ambient modal identification with separated modes. *Journal of Engineering Mechanics*, 137(3):214-226. https://doi.org/10.1061/(ASCE)EM.1943-7889.0000213

Au SK, 2012. Fast Bayesian ambient modal identification in the frequency domain, Part I: posterior most probable value. *Mechanical Systems and Signal Processing*, 26:60-75. https://doi.org/10.1016/j.ymssp.2011.06.017

Au SK, 2014. Uncertainty law in ambient modal identification—Part I: theory. *Mechanical Systems and Signal Processing*, 48(1-2):15-33. https://doi.org/10.1016/j.ymssp.2013.07.016

Au SK, Zhang FL, Ni YC, 2013. Bayesian operational modal analysis: theory, computation, practice. *Computers & Structures*, 126:3-14. https://doi.org/10.1016/j.compstruc.2012.12.015

Brincker R, Ventura CE, 2015. Introduction to Operational Modal Analysis. John Wiley & Sons, Chichester, UK. https://doi.org/10.1002/9781118535141

Brincker R, Zhang LM, Andersen P, 2000. Modal identification from ambient responses using frequency domain decomposition. Proceedings of the International Modal Analysis Conference (IMAC), p.625-630.

Brownjohn JMW, Magalhaes F, Caetano E, et al., 2010. Ambient vibration re-testing and operational modal analysis of the Humber Bridge. *Engineering Structures*, 32(8):2003-2018. https://doi.org/10.1016/j.engstruct.2010.02.034

Doebling SW, Farrar CR, Prime MB, 1998. A summary review of vibration-based damage identification methods. *The Shock and Vibration Digest*, 30(2):91-105. https://doi.org/10.1177/058310249803000201

Felber AJ, 1993. Development of a Hybrid Bridge Evaluation System. PhD Thesis, University of British Columbia, Vancouver, Canada.

Guo J, 2010. Current principal technique status and challenges to be confronted in construction of sea-crossing bridges. *Bridge Construction*, (6):66-69 (in Chinese).

Guo J, Chen Y, Sun BN, 2005. Experimental study of structural damage identification based on WPT and coupling NN. *Journal of Zhejiang University-SCIENCE A*, 6(7):663-669. https://doi.org/10.1631/jzus.2005.A0663

Ibrahim SR, 1977. Random decrement technique for modal identification of structures. *Journal of Spacecraft and*

Rockets, 14(11):696-700.
https://doi.org/10.2514/3.57251

Kim H, Melhem H, 2004. Damage detection of structures by wavelet analysis. *Engineering Structures*, 26(3):347-362.
https://doi.org/10.1016/j.engstruct.2003.10.008

Li BB, Au SK, 2019. An expectation-maximization algorithm for Bayesian operational modal analysis with multiple (possibly close) modes. *Mechanical Systems and Signal Processing*, 132:490-511.
https://doi.org/10.1016/j.ymssp.2019.06.036

Li C, Li HN, Hao H, et al., 2018. Seismic fragility analyses of sea-crossing cable-stayed bridges subjected to multi-support ground motions on offshore sites. *Engineering Structures*, 165:441-456.
https://doi.org/10.1016/j.engstruct.2018.03.066

Liu H, 2006. Hydrodynamic problems associated with construction of sea-crossing bridges. *Journal of Hydrodynamics, Ser. B*, 18(S3):13-18.
https://doi.org/10.1016/s1001-6058(06)60023-1

Liu YC, Loh CH, Ni YQ, 2013. Stochastic subspace identification for output-only modal analysis: application to super high-rise tower under abnormal loading condition. *Earthquake Engineering & Structural Dynamics*, 42(4):477-498.
https://doi.org/10.1002/eqe.2223

Mevel L, Goursat M, Basseville M, 2003. Stochastic subspace-based structural identification and damage detection and localisation—application to the Z24 bridge benchmark. *Mechanical Systems and Signal Processing*, 17(1):143-151.
https://doi.org/10.1006/mssp.2002.1552

Peeters B, de Roeck G, 2001. Stochastic system identification for operational modal analysis: a review. *Journal of Dynamic Systems, Measurement, and Control*, 123(4):659-667.
https://doi.org/10.1115/1.1410370

Ren WX, de Roeck G, 2002. Structural damage identification using modal data. II: test verification. *Journal of Structural Engineering*, 128(1):96-104.
https://doi.org/10.1061/(asce)0733-9445(2002)128:1(96)

Reynders E, Houbrechts J, de Roeck G, 2012. Fully automated (operational) modal analysis. *Mechanical Systems and Signal Processing*, 29:228-250.
https://doi.org/10.1016/j.ymssp.2012.01.007

Sun M, Alamdari MM, Kalhori H, 2017. Automated operational modal analysis of a cable-stayed bridge. *Journal of Bridge Engineering*, 22(12):05017012.
https://doi.org/10.1061/(ASCE)BE.1943-5592.0001141

Taha MMR, Noureldin A, Lucero JL, et al., 2006. Wavelet transform for structural health monitoring: a compendium of uses and features. *Structural Health Monitoring*, 5(3):267-295.
https://doi.org/10.1177/1475921706067741

Xu SQ, Ma RJ, Wang DL, et al., 2019. Prediction analysis of vortex-induced vibration of long-span suspension bridge based on monitoring data. *Journal of Wind Engineering and Industrial Aerodynamics*, 191:312-324.
https://doi.org/10.1016/j.jweia.2019.06.016

Zhang LM, Brincker R, Andersen P, 2005. An overview of operational modal analysis: major development and issues. Proceedings of the 1st International Operational Modal Analysis Conference, p.12.

Zhou Y, Sun LM, 2018. Effects of high winds on a long-span sea-crossing bridge based on structural health monitoring. *Journal of Wind Engineering and Industrial Aerodynamics*, 174:260-268.
https://doi.org/10.1016/j.jweia.2018.01.001

Zhou Y, Sun LM, 2019. Effects of environmental and operational actions on the modal frequency variations of a sea-crossing bridge: a periodicity perspective. *Mechanical Systems and Signal Processing*, 131:505-523.
https://doi.org/10.1016/j.ymssp.2019.05.063

中文概要

题　目：期望最大化贝叶斯模态识别算法在跨海斜拉桥运营模态分析中的应用

目　的：由于地理位置特殊，跨海大桥周围的环境非常复杂，进而导致跨海桥梁的模态特征复杂多变。本文旨在应用期望最大化贝叶斯快速傅里叶变换（FFT）算法对跨海斜拉桥进行运营模态分析。

创新点：1. 通过使用期望最大化贝叶斯 FFT 算法，使得基于贝叶斯的运营模态分析速度更快且收敛性更高；2. 成功识别了 2.5 Hz 以内的 19 阶模态的自然频率、阻尼比以及振型，同时得到了识别参数的不确定性大小。

方　法：通过应用贝叶斯模态识别算法对某跨海斜拉桥的运营模态数据进行分析，并研究模态参数及其不确定性。

结　论：应用期望最大化贝叶斯 FFT 算法能够高效地识别 2.5 Hz 以内的 19 阶模态的自然频率、阻尼比和结构振型，并能得出参数识别的不确定性大小。

关键词：跨海斜拉桥；运营模态分析；期望最大化贝叶斯 FFT 算法